Arch Appl Mech (2009) 79: 41–50
DOI 10.1007/s00419-008-0206-9

ORIGINAL

Ibrahim A. Abbas

Generalized magneto-thermoelasticity in a nonhomogeneous isotropic hollow cylinder using the finite element method

Received: 2 October 2007 / Accepted: 16 January 2008 / Published online: 26 February 2008

Abstract In this paper, we constructed the equations of generalized magneto-thermoelasticity in a perfectly conducting medium. The formulation is applied to generalizations, the Lord–Shulman theory with one relaxation time, and the Green–Lindsay theory with two relaxation times, as well as to the coupled theory. The material of the cylinder is supposed to be nonhomogeneous isotropic both mechanically and thermally. The problem has been solved numerically using a finite element method. Numerical results for the temperature distribution, displacement, radial stress, and hoop stress are represented graphically. The results indicate that the effects of nonhomogeneity, magnetic field, and thermal relaxation times are very pronounced. In the absence of the magnetic field or relaxation times, our results reduce to those of generalized thermoelasticity and/or classical dynamical thermoelasticity, respectively. Results carried out in this paper can be used to design various nonhomogeneous magneto-thermoelastic elements under magnetothermal load to meet special engineering requirements.

Keywords Generalized magneto-thermoelasticity · Nonhomogeneous · Finite element method

1 Introduction

Generalized thermoelasticity theory is receiving the serious attention of researchers, because of the advancement of pulsed lasers, fast burst nuclear reactors, and particle accelerators, etc. that can supply heat pulses with a very fast time rise [1–5]. Chandrasekharaih [6] developed the second sound effect. Now, two different models of generalized thermoelasticity are mainly being extensively used: one proposed by Lord and Shulman (L–S) [7] and the other by Green and Lindsay (G–L) [8]. The L–S theory suggests one relaxation time and, according to this theory, only Fourier's heat conduction equation is modified, whereas the G–L theory suggests two relaxation times and that both the energy equation and the equation of motion are modified. Erbay and Suhubi [9] studied longitudinal wave propagation in an infinite circular cylinder, which is assumed to be made of the generalized thermoelastic material, and thereby obtained the dispersion relation when the surface temperature of the cylinder was kept constant. Generalized thermoelasticity problems for an infinite body with a circular cylindrical hole and for an infinite solid cylinder were solved respectively by Furukawa et al. [10].

Increasing attention is being devoted to the interaction between magnetic fields and strain in a thermoelastic solid due to its many applications in the fields of geophysics, plasma physics, and related topics. In the nuclear field, the extremely high temperatures and temperature gradients as well as the magnetic fields originating inside nuclear reactors influence their design and operation [11]. This is the domain of the theory of magneto-thermoelasticity. It is the combination of two different disciplines: those of the theories of electromagnetism and thermoelasticity. Bahar and Hetnarski [12,13] developed a method for solving coupled thermoelastic problems

I. A. Abbas (✉)
Department of Mathematics, Faculty of Science, Sohag University, Sohag, Egypt
E-mail: ibrahim.abbas@sci.sohag.edu.eg; ibrabbas7@yahoo.com

by using the state-space approach in which the problem is rewritten in terms of the state-space variables, namely the temperature, the displacement, and their gradients. During the last three decades a number of investigations [14–21] have been carried out using the aforesaid theories of generalized thermoelasticity. Note that in most of the earlier studies mechanical or thermal loading on the bounding surface was considered to be in the form of a shock.

The exact solution of the governing equations of the generalized thermoelasticity theory for a coupled and nonlinear/linear system exists only for very special and simple initial and boundary problems. To calculate the solution of general problems, a numerical solution technique is used. For this reason the finite element method is chosen. The method of weighted residuals offers the formulation of the finite element equations and yields the best approximate solutions to linear and nonlinear ordinary and partial differential equations. Applying this method basically involves three steps. The first step is to assume the general behavior of the unknown field variables in such a way as to satisfy the given differential equations. Substitution of these approximating functions into the differential equations and boundary conditions results in some errors, called the residual. This residual has to vanish in an average sense over the solution domain. The second step is the time integration. The time derivatives of the unknown variables have to be determined by former results. The third step is to solve the equations resulting from the first and the second step by using a finite element algorithm program (see Zienkiewicz [22]).

In the present paper, we consider the thermal shock problem of generalized magneto-thermoelasticity of a nonhomogeneous isotropic hollow cylinder. The problem has been solved numerically using a finite element method (FEM). Numerical results for the temperature distribution, displacement, radial stress, and hoop stress are represented graphically. The results indicate that the effects of nonhomogeneity, magnetic field, and thermal relaxation times are very pronounced. A comparison is made with the results predicted by the three theories discussed above.

2 Governing equation

Let us consider an infinite isotropic elastic solid cylinder with internal radius a_1 and external radius a_2. A cylinder coordinate system (r, θ, z) is used for this axisymmetric problem. The cylinder is placed in a constant primary magnetic field H_o, acting in the direction of the z-axis. For a linear, homogenous, and isotropic thermoelastic continuum, the generalized field equations can be presented in a unified form as [19]

$$\sigma_{ij,\,j} + \tau_{ij,\,j} = \rho \ddot{u}_i, \tag{1}$$

$$\left(K_{ij} T_{,\,j}\right)_{,\,i} = \rho C_v \left(\dot{T} + t_0 \ddot{T}\right) + \left(1 + n t_0 \frac{\partial}{\partial t}\right)\left(\gamma T_o \dot{u}_{i,\,i} - \rho Q\right), \tag{2}$$

$$\sigma_{ij} = \lambda u_{i,\,i}\delta_{ij} + \mu\left(u_{i,\,j} + u_{j,\,i}\right) - \gamma\left(T + t_1 \dot{T}\right)\delta_{ij}, \tag{3}$$

$$\tau_{ij} = \mu_o\left(h_i H_j + h_j H_i - h_k H_k \delta_{ij}\right), \tag{4}$$

Where λ and μ are Lame's constants, ρ is the density of medium, C_v is specific heat at constant strain, t is the time, T is the temperature, T_o is the reference temperature, K_{ij} is the thermal conductivity, Q is the heat source, t_0 and t_1 are the relaxation times, δ_{ij} is the Kronecker symbol, σ_{ij} are the components of stress tensor, τ_{ij} are the components of Maxwell stress tensor, u_i are the components of displacement vector, $\gamma = (3\lambda + 2\mu)\alpha_t$, α_t is the coefficient of linear thermal expansion, μ_o is the magnetic permeability, and h_i and H_o are the perturbed and applied magnetic fields, respectively. These equations reduce to the equations of classical dynamical (C–D) coupled theory, Lord and Shulman's theory (L–S), and Green and Lindsay's theory (G–L) as follows

(i) Classical dynamical coupled theory (C–D, 1956)

$$t_0 = 0, \quad t_1 = 0, \quad n = 0.$$

(ii) Lord and Shulman's theory (L–S, 1967)

$$t_0 > 0, \quad t_1 = 0, \quad n = 1.$$

(iii) Green and Lindsay's theory (G–L, 1972)

$$t_0 > 0, \quad t_1 > 0, \quad n = 0.$$

Also, let the magnetic field be such that $\mathbf{H} = \mathbf{H}_o + \mathbf{h}$, where $\mathbf{H}_o = (0,\ 0,\ H_o)$ is the initial magnetic field acting parallel to the z-axis. The Maxwell's equations for the vacuum are

$$\left(\frac{\partial^2}{\partial t^2} - c^2\nabla^2\right)\mathbf{E}^*, \quad \mathbf{h}^* = \mathbf{0}, \quad \text{curl}\left(\mathbf{E}^*,\ \mathbf{h}^*\right) = \frac{1}{c}\frac{\partial}{\partial t}\left(-\mathbf{E}^*,\ \mathbf{h}^*\right). \tag{5}$$

In a cylindrical coordinate system $(r,\ \theta,\ z)$, for the axially symmetric problem, $u_r = u_r(r,\ z,\ t)$, $u_\theta = 0$, $u_z = u_z(r,\ z,\ t)$. Furthermore, if only the axisymmetric plane-strain problem is considered, we have $u_r = u(r,\ t)$ and $u_\theta = u_z = 0$. The strain–displacement relations are

$$e_{rr} = \frac{\partial u}{\partial r}, \quad e_{\theta\theta} = \frac{u}{r}, \quad e_{zz} = e_{rz} = e_{r\theta} = e_{\theta z} = 0. \tag{6}$$

The stress–strain relations are

$$\begin{aligned}
\sigma_{rr} =& 2\mu\frac{\partial u}{\partial r} + \lambda\left(\frac{\partial u}{\partial r} + \frac{u}{r}\right) - \gamma\left(T + t_1\frac{\partial T}{\partial t}\right),\\
\sigma_{\theta\theta} =& 2\mu\frac{u}{r} + \lambda\left(\frac{\partial u}{\partial r} + \frac{u}{r}\right) - \gamma\left(T + t_1\frac{\partial T}{\partial t}\right),\\
\sigma_{zz} =& \lambda\left(\frac{\partial u}{\partial r} + \frac{u}{r}\right) - \gamma\left(T + t_1\frac{\partial T}{\partial t}\right),\ \sigma_{rz} = \sigma_{r\theta} = \sigma_{\theta z} = 0,\\
\tau_{rr} =& \mu_o H_o^2\left(\frac{\partial u}{\partial r} + \frac{u}{r}\right).
\end{aligned} \tag{7}$$

It is assumed that there are no heat sources in the medium, so the equation of motion and energy equation have the form

$$\frac{\partial \sigma_{rr}}{\partial r} + \frac{\sigma_{rr} - \sigma_{\theta\theta}}{r} + \frac{\partial \tau_{rr}}{\partial r} = \rho\frac{\partial^2 u}{\partial t^2}, \tag{8}$$

$$\frac{1}{r}\frac{\partial}{\partial r}(rKT) = \rho C_v\left(\frac{\partial}{\partial t} + t_0\frac{\partial^2}{\partial t^2}\right)T + \gamma T_o\left(\frac{\partial}{\partial t} + nt_0\frac{\partial^2}{\partial t^2}\right)\left(\frac{\partial u}{\partial r} + \frac{u}{r}\right). \tag{9}$$

In this study, we assume that the nonhomogeneous properties of the material are characterized by

$$\lambda = f(r)\,\lambda_*, \quad \mu = f(r)\,\mu_*, \quad \mu_o = f(r)\,\mu_{o*}, \quad \rho = f(r)\,\rho_*, \quad K = f(r)\,K_*, \tag{10}$$

where $f(r)$ is a continuous and nondimensional function and λ_*, μ_*, μ_{o*}, ρ_*, and K_* are the values of λ, μ, μ_o, ρ, and K in the homogeneous case, respectively. Substituting Eq. (10) into Eqs. (7)–(9) we get

$$\begin{aligned}
\sigma_{rr} =& f(r)\left[2\mu_*\frac{\partial u}{\partial r} + \lambda_*\left(\frac{\partial u}{\partial r} + \frac{u}{r}\right) - \gamma_*\left(T + t_1\frac{\partial T}{\partial t}\right)\right],\\
\sigma_{\theta\theta} =& f(r)\left[2\mu_*\frac{u}{r} + \lambda_*\left(\frac{\partial u}{\partial r} + \frac{u}{r}\right) - \gamma_*\left(T + t_1\frac{\partial T}{\partial t}\right)\right],\\
\sigma_{zz} =& f(r)\left[\lambda_*\left(\frac{\partial u}{\partial r} + \frac{u}{r}\right) - \gamma_*\left(T + t_1\frac{\partial T}{\partial t}\right)\right],\ \sigma_{rz} = \sigma_{r\theta} = \sigma_{\theta z} = 0,\\
\tau_{rr} =& \mu_{o*}H_o^2 f(r)\left(\frac{\partial u}{\partial r} + \frac{u}{r}\right),
\end{aligned} \tag{11}$$

$$\begin{aligned}
&f(r)\left[H_a\left(\frac{\partial^2 u}{\partial r^2} + \frac{1}{r}\frac{\partial u}{\partial r} - \frac{u}{r^2}\right) - \gamma_*\frac{\partial}{\partial r}\left(T + t_1\tfrac{\partial T}{\partial t}\right) - \rho_*\frac{\partial^2 u}{\partial t^2}\right]\\
&\quad = -\frac{\partial f(r)}{\partial r}\left[H_a\frac{\partial u}{\partial r} + (H_a - 2\mu_*)\frac{u}{r} - \gamma_*\left(T + t_1\frac{\partial T}{\partial t}\right)\right],
\end{aligned} \tag{12}$$

$$\begin{aligned}
f(r)\left[\frac{\partial^2 T}{\partial r^2} + \frac{1}{r}\frac{\partial T}{\partial r}\right] =& \frac{\partial f(r)}{\partial r}\frac{\partial T}{\partial r} + f(r)\frac{\rho_* C_v}{K_*}\left(\frac{\partial}{\partial t} + t_0\frac{\partial^2}{\partial t^2}\right)T\\
&+ f(r)\frac{T_o\gamma_*}{K_*}\left(\frac{\partial}{\partial t} + nt_0\frac{\partial^2}{\partial t^2}\right)\left(\frac{\partial u}{\partial r} + \frac{u}{r}\right),
\end{aligned} \tag{13}$$

where $H_a = \lambda_* + 2\mu_* + \mu_{o*}H_o^2$, $\gamma_* = (3\lambda_* + 2\mu_*)\alpha_t$. It is convenient to change the preceding equations into a dimensionless form. To do this, the following dimensionless parameters are introduced:

$$T^\circ = \frac{T}{T_o}, \quad (r^\circ,\, u^\circ) = \frac{c}{\chi}(r,\, u), \quad (t^\circ,\, t_o^\circ,\, t_1^\circ) = \frac{c^2}{\chi}(t,\, t_o,\, t_1),$$
$$\left(\sigma_{rr}^\circ,\, \sigma_{\theta\theta}^\circ,\, \sigma_{zz}^\circ,\, \tau_{rr}^\circ\right) = \frac{1}{\mu_*}\,(\sigma_{rr},\, \sigma_{\theta\theta},\, \sigma_{zz},\, \tau_{rr}),$$

with $c^2 = \frac{H_a}{\rho_*}$, $\chi = \frac{K_*}{\rho_* C_v}$, and $f(r) = \left(\frac{r}{\chi/c}\right)^{2m}$ and where m is a rational number. After substitution into Eqs. (11)–(13), one may obtain (after dropping the superscript $^\circ$ for convenience)

$$\begin{aligned}
\sigma_{rr} =& r^{2m}\left[\xi^2\frac{\partial u}{\partial r} + \left(\xi^2 - 2\right)\frac{u}{r} - \eta\left(T + t_1\frac{\partial T}{\partial t}\right)\right],\\
\sigma_{\theta\theta} =& r^{2m}\left[\left(\xi^2 - 2\right)\frac{\partial u}{\partial r} + \xi^2\frac{u}{r} - \eta\left(T + t_1\frac{\partial T}{\partial t}\right)\right],\\
\sigma_{zz} =& r^{2m}\left[\left(\xi^2 - 2\right)\left(\frac{\partial u}{\partial r} + \frac{u}{r}\right) - \eta\left(T + t_1\frac{\partial T}{\partial t}\right)\right],\\
\tau_{rr} =& r^{2m}\omega^2\left(\frac{\partial u}{\partial r} + \frac{u}{r}\right),
\end{aligned} \tag{14}$$

$$\frac{\partial^2 u}{\partial t^2} = \frac{\partial^2 u}{\partial r^2} + \frac{2m+1}{r}\frac{\partial u}{\partial r} + \varepsilon\frac{u}{r^2} - \beta\left(1 + t_1\frac{\partial}{\partial t}\right)\left(\frac{2m}{r}T + \frac{\partial T}{\partial r}\right), \tag{15}$$

$$\frac{\partial^2 T}{\partial r^2} + \frac{2m+1}{r}\frac{\partial T}{\partial r} = \left(\frac{\partial}{\partial t} + t_0\frac{\partial^2}{\partial t^2}\right)T + \varepsilon\left(\frac{\partial}{\partial t} + nt_0\frac{\partial^2}{\partial t^2}\right)\left(\frac{\partial u}{\partial r} + \frac{u}{r}\right), \tag{16}$$

where $\xi^2 = \frac{\lambda_*+2\mu_*}{\mu_*}$, $\omega^2 = \frac{\mu_{o*}H_o^2}{\mu_*}$, $\eta = \frac{T_o\gamma_*}{\mu_*}$, $\varepsilon = 2\left(m - \frac{\mu_*}{H_a}\right) - 1$, $\beta = \frac{T_o\gamma_*}{H_a}$, $\varepsilon = \frac{\gamma_*}{\rho_* C_v}$. From the preceding description, the initial and boundary conditions may be expressed as

$$u(r,\, 0) = \frac{\partial u(r,0)}{\partial t} = 0, \quad T(r,0) = \frac{\partial T(r,0)}{\partial t} = 0, \tag{17}$$

$$\sigma_{rr}(a_1,\, t) = 0, \quad \sigma_{rr}(a_2, t) = 0, \quad T(a_1, t) = H(t), \quad \frac{\partial T(a_2, t)}{\partial r} = 0, \tag{18}$$

where a_1 and a_2 are the inner and outer radii of the hollow cylinder and $H(t)$ denotes the Heaviside unit step function.

3 Finite element method

In order to investigate the numerical solution of thermal shock problem of generalized magneto-thermoelasticity of a nonhomogeneous isotropic hollow cylinder, the FEM [23,24] is adopted due to its flexibility in modeling layered structures and its capability to obtain a full-field numerical solution. The governing Eqs. (15) and (16) are coupled with the initial and boundary conditions (17) and (18). The numerical values of the dependent variables, such as the displacement u and the temperature T, are obtained at the interesting points; these are called degrees of freedom. The weak formulations of the nondimensional governing equations are derived. The set of independent test functions, to consist of the displacement δu and the temperature δT, is prescribed. The governing equations are multiplied by independent weighting functions and then integrated over the spatial domain with the boundary. Applying integration by parts and making use of the divergence theorem to reduce the order of the spatial derivatives allows for the application of the boundary conditions. The same shape functions are defined piecewise on the elements. Using the Galerkin procedure, the unknown fields u and T and the corresponding weighting functions are approximated by the same shape functions. The last step towards the finite element discretization is to choose the element type and the associated shape functions. Three nodes of quadrilateral elements are used. The shape function is usually denoted by the letter N and is usually the coefficient that appears in the interpolation polynomial. A shape function is written for each node of a finite element and has the property that its magnitude is 1 at that node and 0 for all other nodes in that element.

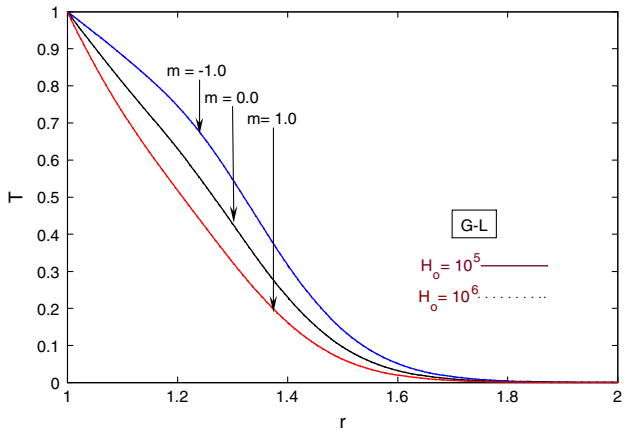

Fig. 1 Variation of temperature for G–L theory at $t = 0.1$ and different values of H_o and m

We assume that the master element has its local coordinates in the range $[-1,1]$. In our case, one-dimensional quadratic elements are used, which are given by:

1. Linear shape functions

$$N_1 = \frac{1}{2}(1-\xi), \quad N_2 = \frac{1}{2}(1+\xi).$$

2. Quadratic shape functions

$$N_1 = \frac{1}{2}\left(\xi^2 - \xi\right), \quad N_2 = 1-\xi^2, \quad N_3 = \frac{1}{2}\left(\xi^2 + \xi\right),$$

On the other hand, the time derivatives of the unknown variables have to be determined by the Newmark time integration method [24].

4 Numerical results

With the view of illustrating and comparing the theoretical results obtained in the previous sections in the context of the C–D, L–S, and G–L theories of thermoelasticity, we now present some numerical results. Copper was chosen as the material for the purposes of numerical computation, the physical data for which are

$$\lambda_* = 7.76 \times 10^{10}(\text{kg})(\text{m})^{-1}(\text{s})^{-2},\ \mu_* = 3.86 \times 10^{10}(\text{kg})(\text{m})^{-1}(\text{s})^{-2},\ T_o = 293(\text{K}),$$
$$\rho_* = 8.954x10^3(\text{kg})(\text{m})^{-3},\ \mu_{o*} = 1\,\text{Gauss(Oersted)}^{-1},\ \alpha_t = 17.8 \times 10^{-6}(\text{K})^{-1},$$
$$K_* = 3.86x10^2(\text{kg})(\text{m})(\text{K})^{-1}(\text{s})^{-3},\ C_v = 3.831x10^2(\text{m})^2(\text{K})^{-1}(\text{s})^{-2},$$

The field quantities, temperature, displacement, and stresses, depend not only on the time t and space r, but also on the nonhomogeneity parameter m, the axial magnetic field H_o, and the thermal relaxation time parameters t_0 and t_1. It has been observed that in all three theories (C–D, L–S, and G–L) the nonhomogeneity parameter m has a significant effect on the field quantities. Here all the variables/parameters are taken in their nondimensional forms. The results for temperature, displacement, radial stress, and hoop stress were obtained out by taking $t = 0.1$ with three different value of m ($m = -1.0,\ 0.0,\ 1.0$) and two different values of H_o ($H_o = 10^5,\ 10^6$). Figures 1, 2, 3, and 4 present the variation of the temperature, displacement, radial stress, and hoop stress with space r under the Green–Lindsay theory (G–L), i.e., when there are two thermal relaxation times ($t_0 = 0.05$, $t_1 = 0.05$, $n = 0$) and for three different values of the nonhomogeneity parameter m with two different value of H_o. Figures 5, 6, 7, and 8 show the variations of the temperature, displacement, radial stress, and hoop stress in all three theories, namely C–D ($t_0 = 0.0$, $t_1 = 0.0$, $n = 0$), L–S ($t_0 = 0.05$, $t_1 = 0.0$, $n = 1$), and G–L ($t_0 = 0.05$, $t_1 = 0.05$, $n = 0$), for two different values of axial magnetic field H_o ($H_o = 10^5$, 10^6) at $m = 1$. Figures 9, 10, 11, and 12 present the variation of the temperature displacement, radial stress,

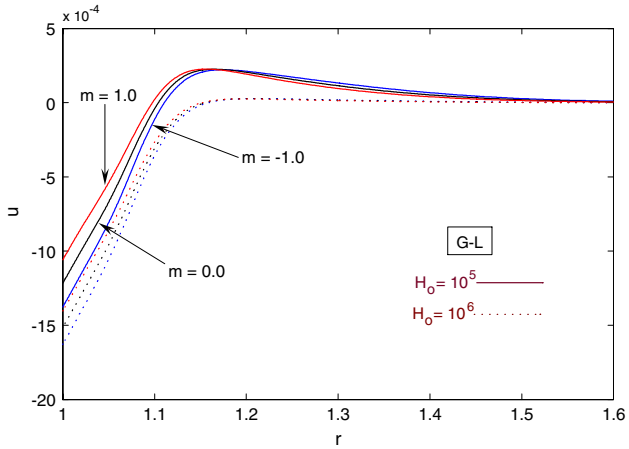

Fig. 2 Variation of displacement for G–L theory at $t = 0.1$ and different values of H_o and m

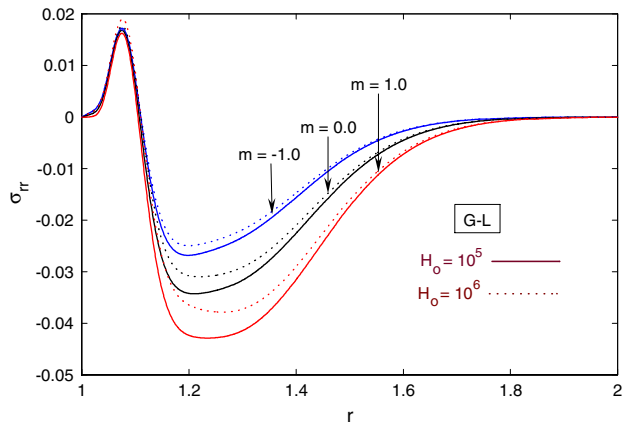

Fig. 3 Variation of radial stress for G–L theory at $t = 0.1$ and different values of H_o and m

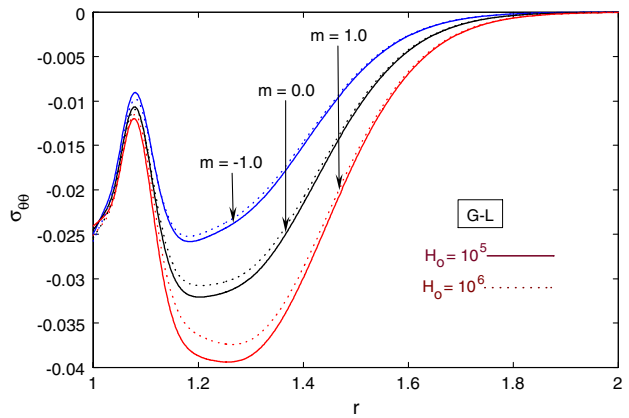

Fig. 4 Variation of hoop stress for G–L theory at $t = 0.1$ and different values of H_o and m

and hoop stress in all the three theories for two different values of nonhomogeneity parameter m ($m = -1.0$, 1.0) at $H_o = 10^6$.

Figures 1, 5, and 9 show the variation of temperature with radial distance in all the three theories, namely C–D, L–S, and G–L. From these figures, one may see that the temperature has a maximum value when $r = a_1$ (which is equal 1) and that this satisfies the boundary conditions. Also, it decreases rapidly with increasing radial distance and vanishes before $r = a_2$ for the three theories, for all the values of m and H_o. Figures 1, 5,

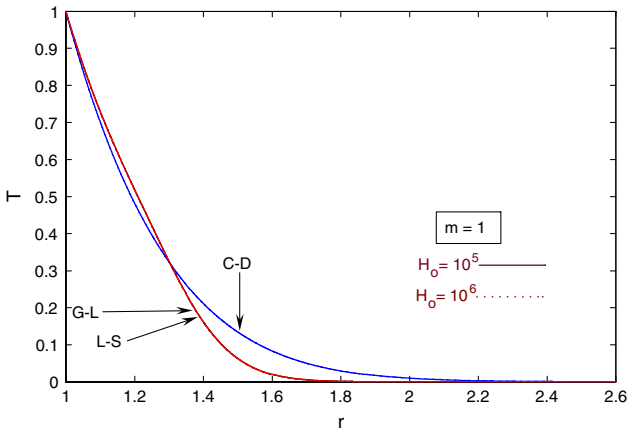

Fig. 5 Variation of temperature for three theories at $t = 0.1$ and different values of H_o

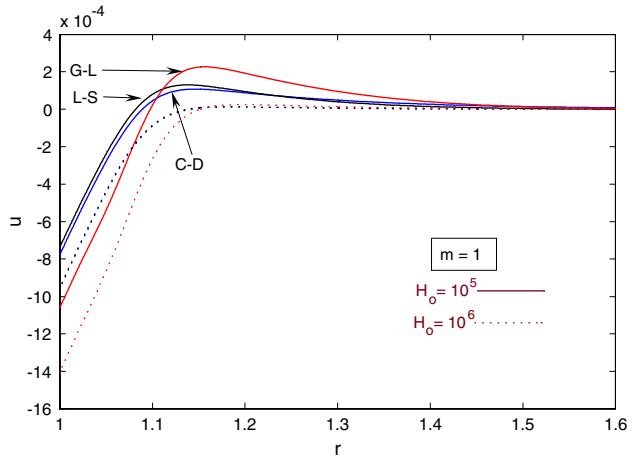

Fig. 6 Variation of displacement for three theories at $t = 0.1$ and different values of H_o

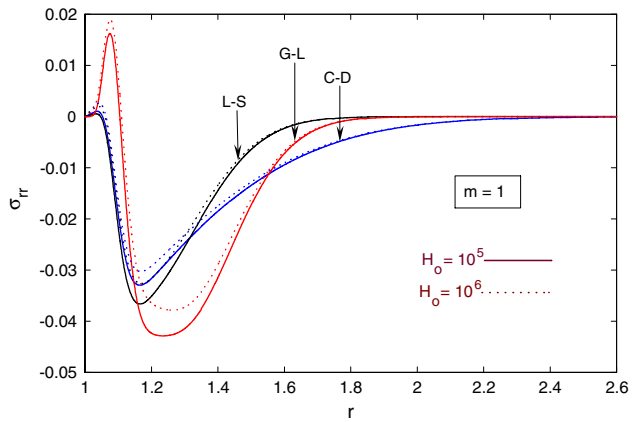

Fig. 7 Variation of radial stress for three theories at $t = 0.1$ and different values of H_o

and 9 demonstrate that there is no significant difference in the values of the temperature for the L–S and G–L theories and with the value of the axial magnetic field H_o.

Figures. 2, 6, and 10 show the variation of the radial displacement with radial distance in all three theories. It is illustrated that the displacement starts with negative values at $r = a_1$, then increases rapidly to positive

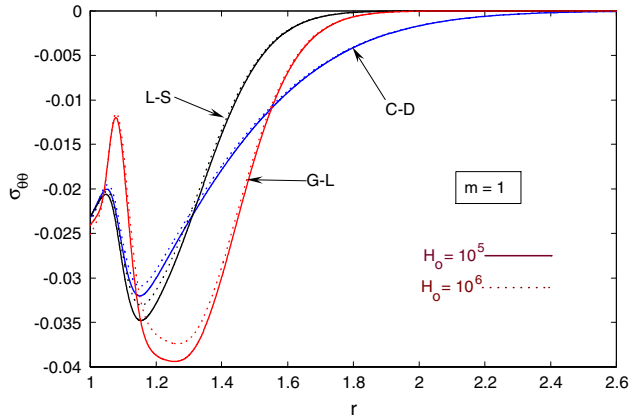

Fig. 8 Variation of hoop stress for three theories at $t = 0.1$ and different values of H_o

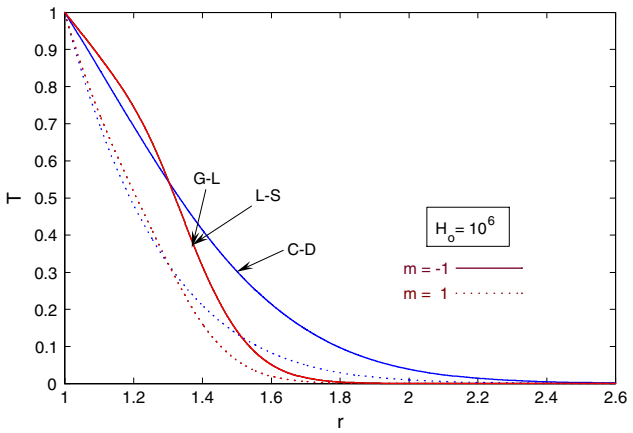

Fig. 9 Variation of temperature for three theories at $t = 0.1$ and different values of m

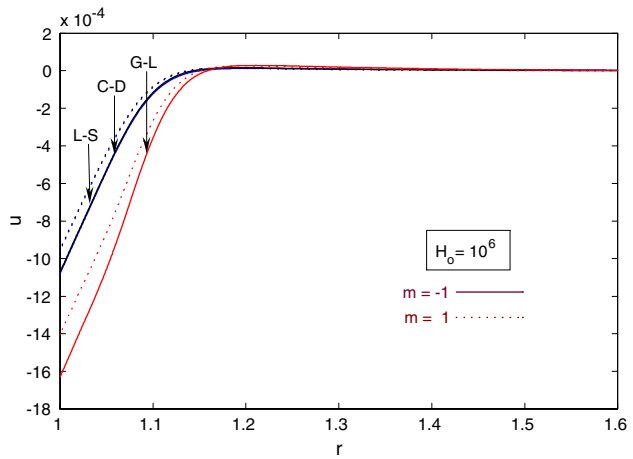

Fig. 10 Variation of displacement for three theories at $t = 0.1$ and different values of m

values. The maximum values of the displacement depend on the values of the time, and the relaxation times for the three theories.

Figures 3, 7, and 11 exhibit the variation of the radial stress with redial distance in all the theories. It is noted that the radial stress increases from zero to a maximum value, after which it decreases rapidly.

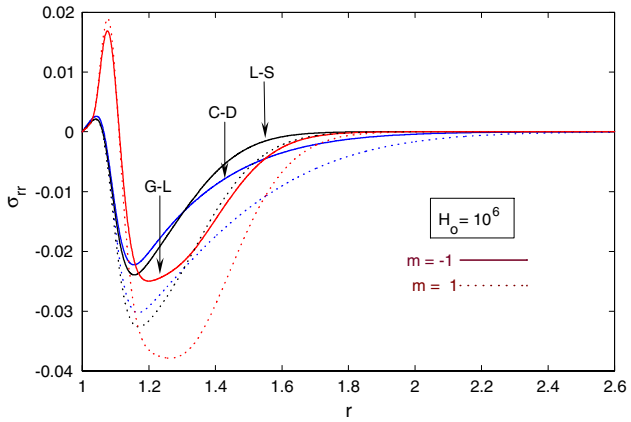

Fig. 11 Variation of radial stress for three theories at $t = 0.1$ and different values of m

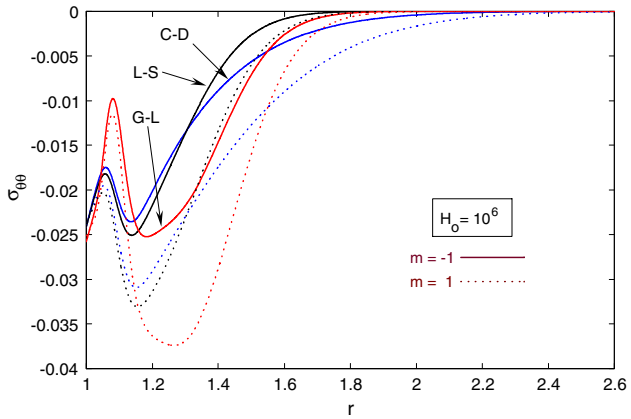

Fig. 12 Variation of hoop stress for three theories at $t = 0.1$ and different values of m

Figures 4, 8, and 12 show that the behavior of the hoop stress with the radial distance changes in the C–D, L–S, and G–L theories in two cases: (i) the hoop stress first decreases sharply, then increases monotonically, afterwards remaining close to zero, (ii) the hoop stress increases sharply to the maximum value, then decreases slowly to the minimum values, after which it increases again monotonically until it remains close to zero.

Finally, It is easily to see that the physical quantities are more sensitive in the G–L theory than in the other two theories, which are almost identical. Furthermore, it has been observed that, in all three theories (C–D, L–S, and G–L), the nonhomogeneity parameter m axial magnetic field H_o and thermal relaxation time parameters t_0 and t_1 have a significant effect on the quantities. The results obtained by the finite element analysis are found to be quite close and are in agreement with analytical and classical solutions given for special cases when $m = 0$ or $H_o = 0$ and $t_0 = t_1 = 0$.

5 Conclusion

A solution of thermal shock problem of generalized magneto-thermoelasticity in a nonhomogeneous isotropic hollow cylinder are presented. The nonhomogeneity of material is characterized by an m value based on the basic material constants. For $m = 0$ the material properties of the cylinder are homogeneous. For $m \neq 0$, the material properties of the cylinder are nonhomogeneous. The thermoelastic responses in the nonhomogeneous cylinder are mainly dependent on the nonhomogeneity properties of material. Therefore, one can design the nonhomogeneity property m of nonhomogeneous structures to decrease the amplitude of thermal stresses in order to satisfy various engineering applications. The problem has been solved numerically using a finite element method. The grid size has been refined and consequently the values of different parameters investigated. Further refinement of the mesh size over 6,000 elements does not change the values considerably, which

is therefore accepted as the grid size for computing purpose. The results show that there is a significant difference in the value of all the variables temperature, displacement, radial stress, and hoop stress with the nonhomogeneity parameter m. We can also observe a large difference between the homogeneous and nonhomogeneous cases.

Acknowledgment The author would like thank the reviewers for their critical review and valuable comments, which improved the paper thoroughly.

References

1. Bargmann, H.: Recent developments in the field of thermally induced waves and vibrations. Nrecl. Eng. Des. **27**, 372 (1974)
2. Anisimov, S.I., Kapeliovich, B.L., Perelman, T.L.: Electron emission from metal surfaces exposed to ultra-short llaser pulses. Sov. Phys. JETP **39**, 375–377 (1974)
3. Boley, B.A.: In: Thermal Stresses: Hasselman, D.P.H., Heller, R.A. (eds.), pp. 1-ll. Plenum, New York (1980)
4. Qiu, T.Q., Tien, C.L.: Heat transfer mechanism during short-pulse laser heating of metals. ASME J. Heat Transf. **115**, 835–841 (1993)
5. Chen, J.K., Beraun, J.E., Tham, C.L.: Ultrafast thermoelasticity for short-pulse laser heating. Int. J. Eng. Sci. **42**, 793–807 (2004)
6. Chandrasekhariah, D.S.: Thermoelasticity with second sound a-review. Appl. Mech. Rev. **39**, 355 (1986)
7. Lord, H., Shulman, Y.: A generalized dynamical theory of thermoelasticity. J. Mech. Phys. Solids **15**, 299–309 (1967)
8. Green, A.E., Lindsay, K.A.: Thermoelasticity. J. Elast. **2**, 1–7 (1972)
9. Erbay, S., Suhubi, E.S.: Longitudinal wave propagation in a generalized thermo-elastic cylinder. J. Therm. Stresses **9**, 279 (1986)
10. Furukawa, T., Noda, N., Ashida, F.: Generalized thermoelasticity for an infinite bode with cylindrical hole. JSME Int. J. **31**, 26 (1990)
11. Nowinski, J.L.: Theory of Thermoelasticity with Applications. Sijthoff & Noordhoff International, Alphen Aan Den Rijn (1978)
12. Bahar, L., Hetnarski, R.: State space approach to thermoelasticity. In: Proceedings of 6th Canadian Congress on Applied Mechanics, pp. 17–18. University of British Columbia, Vancouver (1977)
13. Bahar, L., Hetnarski, R.: Transfer matrix approach to thermoelasticity. In: Proceedings of the 15th Midwest Mechanic Conference, pp. 161–163. University of Illinois, Chicago (1977)
14. Furukawa, T., Noda, N., Ashida, F.: Generalized thermoelasticity for an infinite bode with cylindrical hole. JSME Int. J. **31**, 26 (1990)
15. Sharma, J.N., Chand, D.: On the axisymmetrical and plane strain problems of generalized thermoelasticity. Int J. Eng. Sci. **30**, 223–230 (1992)
16. Chandrasekharaiah, D.S., Murthy, H.N.: Thermoelastic interactions in an unbounded body with a spherical cavity. J. Therm. Stresses **16**, 55–71 (1993)
17. Misra, J.C., Chattopadhyay, N.C., Samanta, S.C.: Thermoviscoelastic waves in an infinite aeolotropic body with a cylindrical cavity-a study under the review of generalized theory of thermoelasticity. Comp. Struc. **52**(4), 705–717 (1994)
18. Chandrasekharaiah, D.S.: One-dimensional wave propagation in the linear theory of thermoelasticity with energy dissipation. J. Therm. Stresses **19**, 695–710 (1996)
19. Abd-alla, A.N., Abbas, I.A.: A problem of generalized magnetothermoelasticity for an infinitely long, perfectly conducting cylinder. J. Therm. Stresses **25**, 1009–1025 (2002)
20. Misra, J.C., Samanta, S.C., Chakraborty, A.K., Misra, S.C.: Magnetothermoelastic interaction in an infinite elastic continuum with a cylindrical hole subjected to ramp-type heating. Int. J. Eng. Sci. **29**(12), 1505–1514 (1991)
21. Misra, J.C., Samanta, S.C., Chakraborty, A.K.: Magnetothermoelastic interaction in an aeolotropic solid cylinder subjected to a ramp-type heating. Int. J. Eng. Sci. **29**(9), 1065–1075 (1991)
22. Zienkiewicz, O.C., Taylor, R.L.: The Finite Element Method Fluid Dynamics, 5th edn. Butterworth-Heinemann, London (2000)
23. Reddy, J.N.: An Introduction to the Finite Element Method, 2nd edn. McGraw-Hill, New York (1993)
24. Cook, R.D., Malkus, D.S., Plesha, M.E.: Concepts and Applications of Finite Element Analysis, 3rd edn. Wiley, New York (1989)